



Adsorption effect and mechanism of Cd(II) by different phosphorus-enriched biochars

Yang Zeng¹ · Yuhan Lin¹ · Ming Ma^{1,2,3} · Hong Chen^{1,2,3}

Received: 21 November 2023 / Accepted: 29 January 2024 / Published online: 6 February 2024
© The Author(s), under exclusive licence to Springer-Verlag GmbH Germany, part of Springer Nature 2024

Abstract

The resource utilization of agricultural and forestry waste, especially the high-value transformation of low-grade phosphate rock and derivatives, is an important way to achieve sustainable development. This study focuses on the impregnation and co-pyrolysis of rice straw (RS) with fused calcium magnesium phosphate (FMP), FMP modified with citric acid (CA-FMP), and calcium dihydrogen phosphate (MCP) to produce three phosphorous-enriched biochars (PBC). The Cd(II) removal efficiency of biochars before and after phosphorus modification was investigated, along with the adsorption mechanism and contribution of biochars modified with different phosphorus sources to Cd(II) adsorption. The result indicated that CA-FMP and MCP could be more uniformly loaded onto biochar, effectively increasing the specific surface area (SSA) and total pore volume. The adsorption of Cd(II) onto PBC followed a mono-layer chemisorption process accompanied by intraparticle diffusion. The adsorption of Cd(II) by PBC involved ion exchange, mineral precipitation, complexation with oxygen-containing functional groups (OFGs), cation- π interaction, electrostatic interaction, and physical adsorption. Ion exchange was identified as the primary adsorption mechanism for Cd(II) by BC and FBC (51.53% and 53.15% respectively), while mineral precipitation played a major role in the adsorption of Cd(II) by CBC and MBC (51.10% and 47.98% respectively). Moreover, CBC and MBC significantly enhanced the adsorption capacity of Cd(II), with maximum adsorption amounts of 128.1 and 111.5 mg g⁻¹ respectively.

Keywords Phosphorous-enriched biochar · Agricultural and forestry waste · Low-grade phosphate rock and derivatives · Cadmium · Adsorption mechanism · Mineral precipitation

Introduction

Cd(II) contamination in water poses significant threats to both food safety and human health, given its bioaccumulation and prolonged presence in the food chain (Zhang et al. 2023). The China Drinking Water Quality Standard (GB5749-2022) stipulates that the maximum allowable

concentration of Cd(II) is 0.005 mg L⁻¹. Even low concentrations of Cd(II) can induce the generation of free radicals in the human body, leading to protein, lipid, and DNA damage, thereby causing various health issues (Zhang et al. 2017). Therefore, it is important to develop simple and efficient products to remove Cd(II) from wastewater. At present, the methods for removing Cd(II) from wastewater mainly include adsorption, chemical precipitation, flocculation, membrane separation, ion exchange, and electric remediation (Zamora-Ledezma et al. 2021). Biochar has become the mainstream choice for heavy metal adsorption remediation due to its high adsorption efficiency and cost performance (Shrestha et al. 2021).

Phosphorus modification exerts effective control over the mineral composition and pore distribution of biochar, enhancing its capacity to adsorb, precipitate, and complex Cd(II) (Huang et al. 2022). The categories and properties of phosphorus precursors play a vital role in influencing the adsorption performance, phosphorus form, and

Responsible Editor: Tito Roberto Cadaval Jr

✉ Hong Chen
chenhong@swu.edu.cn

¹ College of Resources and Environment, Southwest University, Chongqing 400715, China

² Chongqing Engineering Research Center for Agricultural Non-Point Source Pollution Control, Three Gorges Reservoir Area, Chongqing 400715, China

³ Chongqing Key Laboratory of Agricultural Resources and Environment, Chongqing 400715, China

availability of PBC. Numerous studies have utilized K_3PO_4 as a representative water-soluble phosphorus precursor and hydroxyapatite as a representative insoluble phosphorus precursor. Zhang et al. (Zhang et al. 2022a) found that the maximum adsorption of Cd(II) by PBC modified by K_3PO_4 was 6.6 times that of the original biochar. Chen et al. (Chen et al. 2021) demonstrated that the adsorption capacity of Cd(II) was significantly increased by electrostatic interaction, ion exchange, and functional group complexation of PBC loaded with hydroxyapatite. However, information on the utilization of citrate-soluble phosphates as a phosphorus source for the preparation of PBC and its application in the remediation of Cd(II) contaminated water bodies is limited.

In light of the rapid depletion of global phosphorus resources, China possesses a mere 4.5% retention rate of phosphate ore worldwide, yet astonishingly accounts for 57% of the mined quantity (Yu and Du 2023). The medium and low-grade phosphate rock constitute approximately 90% of the total. The primary means of utilizing it entails the extraction and refinement of phosphate ores to yield water-soluble phosphates, such as MCP. Nevertheless, this approach is accompanied by certain drawbacks, including substantial energy consumption, resource wastage from tailings, and environmental risks. Given the significant reliance of industrial and agricultural on phosphate rock resources, the cost-effective citrate-soluble phosphorus source derived from medium and low-grade phosphate rock and its derivatives has emerged as a research focus for achieving its high-value utilization (Zhao et al. 2018). Furthermore, it is anticipated that impurity elements present in citrate-soluble phosphorus sources could contribute to the functionalization process of PBC. However, there is a dearth of studies on the preparation of PBC using citrate-soluble phosphorus sources as exogenous phosphorus. FMP is a kind of alkaline phosphorus source containing a large amount of citrate-soluble phosphorus and a variety of medium and trace elements (Ca, Mg, and Si). However, its chemical stability is relatively low, whereas the thermal stability of the phosphate-containing silicate glass is exceptionally high, rendering direct doping onto the biochar surface impractical. To address this, the addition of CA as an activator is crucial, as it reduces the size of FMP, disrupts the silica tetrahedral network, and exposes the mineral elements, thereby enhancing the loading effect of FMP (Xu et al. 2010).

In this study, three different phosphorus precursors, namely FMP, CA-FMP, and MCP, were selected for the phosphorus modification of biochar, with BC serving as the control. The synthesis of three distinct PBCs was achieved through impregnation and co-pyrolysis of RS and the aforementioned phosphorus precursors. The influence of different phosphorus precursors on the physicochemical properties of

PBC was analyzed, and the adsorption mechanism of Cd(II) was studied. This research provides a theoretical foundation for the remediation of cadmium-polluted water bodies through the application of PBC, as well as the innovative utilization of derivatives from medium and low-grade phosphate rock.

Materials and methods

Preparation of PBC

RS were collected from farmland in Chongqing, China. The samples underwent a series of procedures including washing with deionized water, drying, crushing, and sifting through an 80-mesh screen, then placed in a dryer for use. PBC is prepared by impregnation and co-pyrolysis. To be specific, the RS soaked in 2% FMP solution ($m:v = 1:10$), 2% MCP solution, 2% FMP + 2% CA solution, respectively. After undergoing electromagnetic stirring impregnation for 2 h, and the mixture was dried in oven at 378 K for 24 h. Then, the precursor was placed in a porcelain crucible for co-pyrolysis in a tube furnace. The whole pyrolysis process under the CO_2 flow ($50 \text{ mL}\cdot\text{min}^{-1}$), and the temperature was raised to 773 K at a rate of $5 \text{ K}\cdot\text{min}^{-1}$, kept for 2 h. Three kinds of PBC prepared with FMP, CA-FMP and MCP as sources of phosphorus were named FBC, CBC and MBC, respectively. And RS was pyrolyzed to produce the original biochar as a control, which was named BC.

Material characterization

The pH of biochars were determined after mixing 18 h in 5% ($w\cdot v^{-1}$) suspension in deionized water (Deng et al. 2020). The zeta potential (ζ) of biochars was measured by Zeta potential analyzer (Mastersizer 3000, PANalytical, Netherlands). The volatile (V_{ad}), ash (A_{ad}), and fixed carbon (FC_{ad}) contents of biochars were characterized according to Charcoal and Charcoal Test Method (GB/T 17664–1999). The CHN/O element analyzer (Flashsmart, Thermo Fisher Scientific Inc, Italy) was used to determine the C, N, and H content on biochars, and the O content is calculated by applying a mass balance. The SSA and pore distribution of biochar were evaluated by a multilayer isothermal adsorbent (ASAP 2460, Micromeritics, USA), and the SSA and pore information were determined by BET equation. The surface morphology and element distribution of biochar were observed by field emission scanning electron microscope and energy spectrum analyzer (Sigma 500, Carl Zeiss AG, Britain). The crystalline structure of biochar before and after adsorption of Cd(II) was obtained by X-ray diffraction (XRD, XPert Powder, PANalytical, Netherlands) using

CuK α radiation. The Fourier transform infrared (FTIR, VERTEX 70, Bruker, Germany) spectrum of biochars was used to observe the surface functional group composition of biochars before and after adsorption of Cd(II) in the range of 400–4000 cm^{-1} .

Adsorption experiments and data analysis

In the adsorption experiment, 20 mg biochar was mixed with 25 mL $\text{Cd}(\text{NO}_3)_2$ solution (containing $0.01 \text{ mol}\cdot\text{L}^{-1}$ NaNO_3 , 150 rpm, 10 h, 298 K). The suspension was filtered by the 0.45- μm filter membrane; the concentrations of Cd(II) are determined by ICP-OES (Optima 7000 DV, PerkinElmer, USA). To observe the effects of coexisting cation and pH concentration on adsorption, the experimental parameters were adjusted accordingly. Isothermal adsorption and adsorption kinetics experiments were conducted. In the adsorption kinetics experiment, the sample was analyzed using the UV–VIS spectrophotometer (Thermo Scientific EVO 60, Thermo Fisher Scientific Inc., Italy) to determine the soluble orthophosphate (Soluble Or-P), polyphosphate (Py-P) and total phosphorus (TP) from biochar (Sun et al. 2018). Regeneration and reuse studies were conducted on biochars for the removal of Cd(II) over 4 consecutive adsorption–desorption cycles. The data of adsorption kinetics were fitted using the pseudo-first-order (PFO), pseudo-second-order (PSO), and intra-particle diffusion (IPD) models (Lang et al. 2023; Wang et al. 2023). The data of isothermal adsorption were fitted using the Langmuir and Freundlich models (Zhou et al. 2023). Detailed steps can be found in Supplementary Information.

Quantitative analysis of different mechanisms to biochar adsorption of Cd(II)

Impregnate the biochar in 1 M HCl for 24 h, and rinse with deionized water until the solution pH is constant, then dry for 24 h to obtain the demineralized biochar (Cui et al. 2016). The effect of minerals in biochar on the adsorption of Cd(II) was eliminated by demineralization. 20 mg biochar and

demineralized biochar sample was mixed with 20 mL 50 mg L^{-1} $\text{Cd}(\text{NO}_3)_2$ solution, the suspension was extracted and filtered, and then use ICP-OES to determine concentration of Cd(II), K(I), Na(II), Ca(II), and Mg(II). With reference to the method proposed by Zhang et al. (Zhang et al. 2022b), different mechanisms of adsorption of Cd(II) by PBC were quantitatively analyzed. Detailed steps can be found in Supplementary Information.

Results and discussion

Characterization of PBC

Since phosphorus is enriched in ash during pyrolysis, it also catalyzes the further aromatization of biochar and forms more abundant OFGs (Zhang et al. 2020b). The addition of mineral elements increased the A_{ad} content of PBC, while reducing the V_{ad} and FC_{ad} content, as well as decreasing the proportion of C and H (Table 1). The pH of PBC is mainly related to the acidity and alkalinity of its precursor. In particular, the addition of CA increases the pH of PBC, possibly because CA is consumed in the process of activating FMP and biomass, and the alkaline cation released after activation is retained into biochar in the form of ash, and the remaining CA is converted into CO_3^{2-} or CO_2 during the pyrolysis process.

Uneven size FMP fragments are distributed on the surface of FBC (Fig. 1), which may lead to the blockage of biochar pore channels and the obstruction of pore formation during the pyrolysis process, resulting in lower SSA and total pore volume than BC. CA can reduce the size of FMP by disrupting its chemical unstable structure, thereby addressing the issue of blockage. The products generated after activation are respectively silicon short chains and mineral elements (Ca, Mg, Si, and P) entering the solution (Hou et al. 2019). Alkali metal ions uniformly loaded on biomass through impregnation, can decompose macromolecular tar fragments via heterolytic mechanism under high-temperature conditions. This process increases the formation of low molecular weight substances, inhibits the escape

Table 1 Physicochemical properties of biochars

Biochar	pH	Composition (%)			Elemental content (%)				SSA ($\text{m}^2\cdot\text{g}^{-1}$)	Total pore volume ($\text{cm}^3\cdot\text{g}^{-1}$)	Average pore size (nm)
		V_{ad}	A_{ad}	FC_{ad}	C	H	O	N			
BC	10.47 ± 0.10	0.336	0.345	0.319	44.80	18.30	17.24	1.45	39.82	0.072	12.56
FBC	10.18 ± 0.14	0.171	0.639	0.19	18.37	0.86	16.21	0.52	28.14	0.059	14.27
CBC	10.66 ± 0.01	0.157	0.563	0.28	24.29	1.12	17.75	0.47	123.28	0.150	7.44
MBC	6.99 ± 0.16	0.269	0.455	0.276	38.56	1.53	15.20	1.22	65.97	0.102	2.86

O content is obtained by differential subtraction, $\text{O}\% = 1 - \text{C}\% - \text{H}\% - \text{N}\% - \text{Ash}\%$

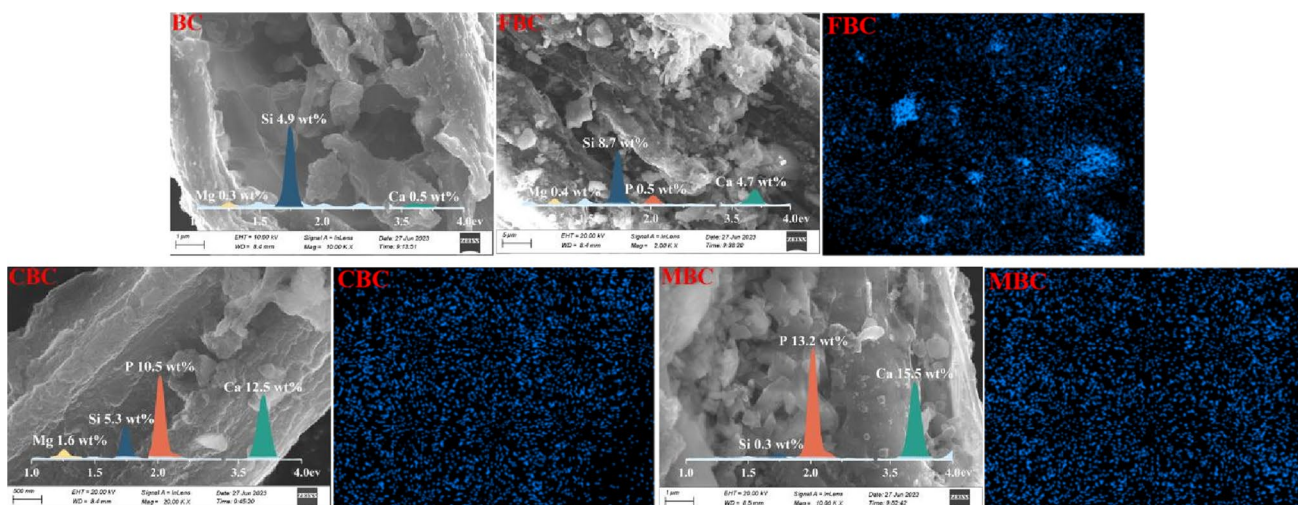


Fig. 1 SEM-EDS of origin and phosphorus-enriched biochars

of gaseous tar molecules, and leads to formation of denser and more porous biochar (Feng et al. 2018; Yu et al. 2013). Additionally, CA and the intermediate products HPO_4^{2-} and HSiO_4^{3-} provide H^+ to catalyze the formation of micropores. The carbon skeleton is protected through cyclization or dehydration condensation, and cross-linked phosphate with biochar to avoid pore collapse caused by micropore formation (Chu et al. 2018). The SSA and total pore volume of CA-FMP and MCP modified biochar increase significantly. Meanwhile, the surface of PBC is rougher than that of BC, and more abundant pore structure is formed. As a result, the surface of CBC and MBC possess a great number of active binding sites, allowing for more uniform and increased loading of phosphorus (Fig. 1).

Behaviors of Cd(II) adsorption on PBC

Adsorption kinetics

The adsorption rates of Cd(II) by biochars initially increased and then gradually decreased, reaching equilibrium at approximately 300 min (Fig. 2a). The equilibrium adsorption amounts were 7.828, 14.582, 44.879, and 34.544 mg g^{-1} , respectively (Table 2). Compared with BC, the adsorption rate of PBC was significantly higher and the equilibrium time was shorter, which is consistent with the comparison of K_1 and K_2 value in the PSO and PFO adsorption kinetics. PBC exhibited a higher fitting degree in PFO adsorption kinetics, and the theoretical adsorption capacity closely

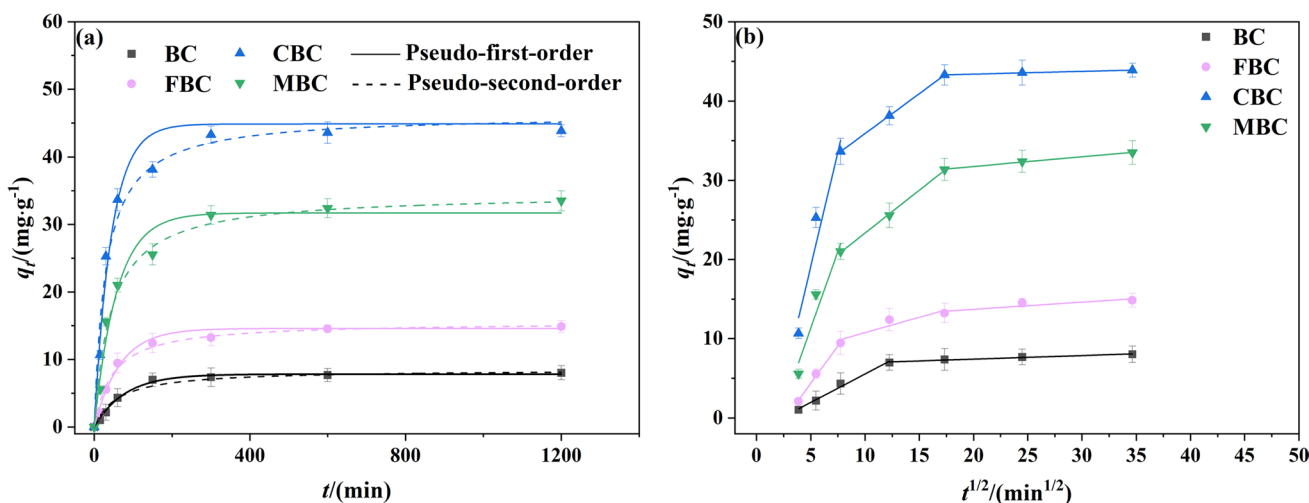


Fig. 2 PFO and PSO adsorption kinetics (a) and IPD adsorption kinetics (b) of biochars for Cd(II)

Table 2 PFO and PSO adsorption kinetics parameters of biochars for Cd(II)

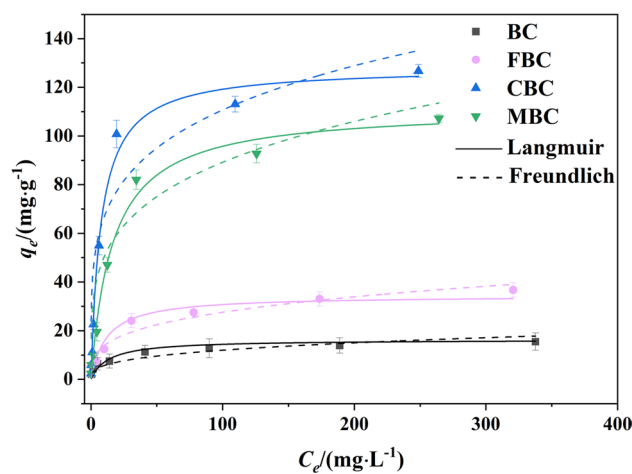
Biochar	Pseudo-first-order adsorption kinetics			Pseudo-second-order adsorption kinetics					
	$K_1/(\text{min}^{-1})$	$q_{t,cal}/(\text{mg g}^{-1})$	R^2	$K_2/(\text{g g}^{-1} \text{min}^{-1})$	$q_{t,cal}/(\text{mg g}^{-1})$	R^2			
BC	0.017	7.828	0.993	0.137	8.523	0.976			
FBC	0.017	14.582	0.979	0.193	15.533	0.992			
CBC	0.023	44.879	0.970	0.727	34.544	0.984			
MBC	0.018	34.544	0.975	0.657	46.277	0.980			
Biochar	Internal diffusion adsorption kinetics								
	$K_{ip1}/(\text{mg g}^{-1} \text{min}^{-1})$	C_1	R^2	$K_{ip2}/(\text{mg g}^{-1} \text{min}^{-1})$	C_2	R^2	$K_{ip1}/(\text{mg g}^{-1} \text{min}^{-1})$	C_3	R^2
BC	0.717	-1.620	0.989	0.045	6.524	0.968	-	-	-
FBC	1.888	-5.055	0.997	0.390	6.844	0.884	0.089	11.927	0.822
CBC	5.785	-9.770	0.901	1.007	25.837	0.998	0.034	42.716	0.991
MBC	3.882	-8.061	0.929	1.083	12.505	0.998	0.122	29.314	0.991

matched the experimental adsorption capacity, indicating that the adsorption process is primarily driven by chemical adsorption (Ho and McKay 1999). This also suggests that adsorption performance of PBC is mainly attributed to ion exchange and mineral precipitation.

By fitting the IPD model, it was observed that the mass transfer process of Cd(II) in PBC can be divided into three stages: film diffusion, intraparticle diffusion, and the adsorption onto active sites (Fig. 2b) (Wang and Guo 2022). Compared with BC, the K_{ip} value and C value of PBC were increased, indicating enhanced diffusion in the liquid film surrounding PBC, transfer within the pores of PBC and adsorption onto the active sites of PBC (Yuan et al. 2023). The intercepts in the IPD model were not zero, indicating that the rate determining step was not only the IPD process, but also the chemisorption process (Wu et al. 2021).

Adsorption isotherms

As the initial concentration of Cd(II) increased, the adsorption onto the biochars increased rapidly and then gradually slowed down until reaching adsorption equilibrium (Fig. 3). The fitting of Langmuir model and Freundlich model revealed that the adsorption process of Cd(II) is characterized mono-layer molecular adsorption and is highly controlled by chemisorption process (Yang et al. 2023). The adsorption characteristic constant K_L of the Langmuir isothermal model falls within the range of 0 to 1, signifying the favorable adsorption capacity of biochars on Cd(II). Similarly, the linear constant $1/n$ of the Freundlich isothermal model is found to be less than 1, further supporting the notion of biochar's effective adsorption capability towards Cd(II). The results of the two models constant K_L and K_F are $\text{CBC} > \text{MBC} > \text{FBC} > \text{BC}$, indicating that the distribution of effective adsorption sites on the surface of PBC is more uniform and abundant (Meng and Hu 2021). Additionally, the

**Fig. 3** Adsorption isotherms of biochars for Cd(II)

maximum adsorption capacity of PBC fitted by the Langmuir isothermal model was significantly higher than that of BC (Table 3), which was 2.11, 7.86, and 6.84 times of the maximum adsorption capacity of BC, respectively, demonstrating that phosphorus modification significantly enhanced the adsorption capacity of biochar for Cd(II). In addition, the CBC in this study exhibited Cd removal capabilities that were comparable to, or even surpassed, conventional biochar (Table S1).

Adsorption mechanism analysis

CA modification enables more diverse mineral composition to participate in Cd co-precipitation

In order to understand the mineral types of modified biochars using different phosphorus sources and the adsorption contribution of mineral precipitation to the removal of Cd(II)

after adsorption of Cd(II) varied (Fig. 5b). It was found that MBC has a higher total phosphorus content and Py-P proportion (61.74%), while CBC has a higher Soluble Or-P proportion (60.64%), leading to differences in mineral composition and the type of Cd(II) precipitation. The lower total phosphorus content and phosphorus recovery rate (83.6%) in CBC may be due to the conversion of HPO_4^{2-} to P_2O_5 or PH_3 loss through volatilization under high temperature conditions (Bruun et al. 2017; Zhang et al. 2021). The high concentration of phosphorus load is considered to be the main factor for effective removal of Cd(II) from PBC (Wang et al. 2022). This result was confirmed by the detection of PO_4^{3-} release curve by PBC and the content of PO_4^{3-} after Cd(II) adsorption (Fig. 6). PO_4^{3-} in biochars is rapidly released within 0–6 h and reaches equilibrium concentration after 20 h, which is consistent with the removal trend of Cd(II) in adsorption kinetics. From the PO_4^{3-} content after adsorption of Cd(II), it can be found that the equilibrium PO_4^{3-} concentration decreases significantly with the increase of the initial Cd(II) concentration, and PO_4^{3-} drops below 5 mg L^{-1} at the initial Cd(II) concentration of 100 mg L^{-1} , indicating a minimal risk of eutrophication caused by PBC in practical applications. Moreover, P plays a crucial role in Cd(II) adsorption by PBC, which is consistent with the findings from FTIR analysis (Fig. 7). Peaks near 565 cm^{-1} , 602 cm^{-1} , and 980 cm^{-1} were observed in PBC, which could prove the existence of dicalcium phosphate, hydroxyapatite and tricalcium phosphate, respectively. The peak generated near 1090 cm^{-1} represents P-O-P in pyrophosphate, and the peak value at 539 cm^{-1} is related to the antisymmetric PO_4^{3-} variable angle vibration (Bekiaris et al. 2016; Zhang et al. 2022b). The absorption peaks of the above groups weaken or shift after Cd(II) adsorption, indicating co-precipitation reactions between the phosphate-containing functional groups and Cd(II).

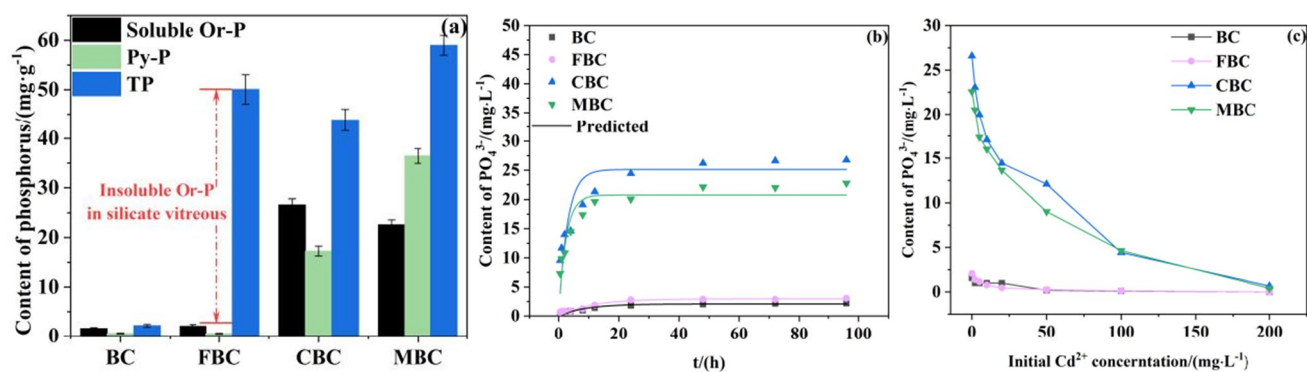


Fig. 6 Phosphorus form (a), PO_4^{3-} release kinetics curve (b), and PO_4^{3-} content after adsorption of Cd(II) (c) of biochars

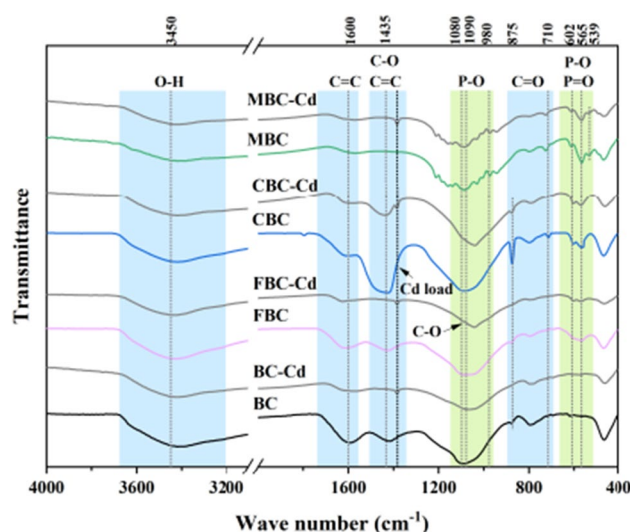


Fig. 7 FTIR diagram of biochars before and after Cd(II) adsorption

Impurity metals in citrate-soluble phosphorus source dominate ion exchange

Ion exchange is another important mechanism for the adsorption of Cd by PBC. The Q_i of BC, FBC, CBC, and MBC were 4.029, 7.721, 15.198, and 12.266 mg g^{-1} , respectively (Table 4). Among them, the initial concentration and net release of bivalent cations are higher, leading to a greater adsorption of Cd(II) through ion exchange. The ion exchange process involves the electrostatic interaction of metal ions to the negatively charged potential on the biochar surface, and through electrostatic gravitational action, Cd(II) occupies the original binding site of metal ions, forming R-COO-Cd, R-O-Cd, or Cd(II) replaces Ca(II) and Mg(II) to precipitate on biochar (Deng et al. 2019). In solution, K(I) and Na(I) have low charge density and large ionic radius, making them unable to form complexes. They remain stable and

Table 4 Ion release before and after adsorption of Cd(II) and Total Cd(II) adsorbed by origin and phosphorus-enriched biochars

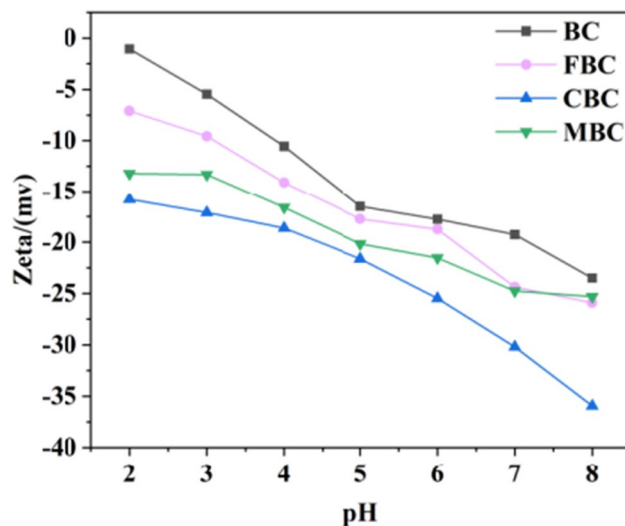
Biochar	The net amounts of released cations (mg·g ⁻¹)				Total Cd(II) adsorbed (mg·g ⁻¹)
	Ca(II)	Mg(II)	K(I)	Na(I)	
BC	0.869 ± 0.007	0.183 ± 0.003	0.122 ± 0.005	0.057 ± 0.002	4.029 ± 0.044
FBC	1.918 ± 0.013	0.407 ± 0.021	0.079 ± 0.002	0.035 ± 0.006	7.721 ± 0.027
CBC	2.646 ± 0.009	1.448 ± 0.017	0.169 ± 0.003	0.107 ± 0.003	15.198 ± 0.156
MBC	3.383 ± 0.006	0.437 ± 0.038	0.133 ± 0.011	0.051 ± 0.003	12.266 ± 0.099

resistant to hydrolysis in solution. On the other hand, Ca(II) and Mg(II) are more prone to form spherical complexes in solution, further facilitating ion exchange (Shang et al. 2020; Zhang et al. 2022b). This is consistent with our findings; the addition of excessive Na(I) as coexisting cations does not impact the adsorption of cadmium. However, an excessive Ca(II) competes with cadmium for adsorption sites, leading to the inhibition of cadmium adsorption (Fig. S1a). Hence, these alkaline earth metal elements, typically considered impurities in the phosphate refining process, are loaded onto biochar following CA activation, becoming a significant factor in promoting the adsorption capacity of Cd(II).

OFG complexation and other mechanisms

The OFGs are an important factor affecting the adsorption of heavy metals on biochar. The OFGs (such as R-OH, R-COOH, etc.) on the surface of biochar are complexed with Cd(II), and the released H⁺ is the main reason for the decrease of solution pH (Wang et al. 2022). After adsorption of Cd(II), the FTIR diagram (Fig. 7) reveals a weakening of the peak intensity for the -OH vibration peak (3415–3430 cm⁻¹) and the C–O–C vibration peak (1070–1080 cm⁻¹) (Zhang et al. 2022b). Additionally, a new vibration peak emerges at 1385 cm⁻¹, possibly due to the complexation of OFGs on the surface and their participation in the removal of Cd(II) (Deng et al. 2020).

The potential mechanism underlying the adsorption of Cd(II) by PBC also encompasses cation- π interaction, electrostatic interaction, physical adsorption, etc. (Liu et al. 2022). The peak strength of the C=C bond around 1600 cm⁻¹ and the aromatic C-H bond around 710–845 cm⁻¹ changes after Cd(II) adsorption (Fig. 7), which is regarded as the contribution of cation- π interaction to the removal of Cd(II) (Cui et al. 2016). The electrostatic interaction capacity is mainly related to the zeta value of biochar. A higher the absolute value of negative potential indicates that the surface of biochar has more negative charge and stronger electrostatic attraction (Zhang et al. 2020a). The zeta values of both BC and PBC are less than 0 (Fig. 8), which proves that they have good electrostatic interaction capacity. With the increase of pH, the surface acid groups

**Fig. 8** Zeta diagram of biochars

of biochar are dissociated or ionized, the surface negative charge is further increased, and the electrostatic interaction force of biochar is increased. This is consistent with our findings that in the pH range of 2–8, an increase in pH values resulted in an elevation of the adsorption capacity of biochar (Fig. S1b). The absolute values of zeta value of the biochar modified with phosphorus increased, and the number of Cd(II) adsorbed by electrostatic interaction was ranked as CBC > MBC > FBC > BC. The physical adsorption capacity is mainly determined by pore structure and SSA, which affect the adsorption site of biochar surface (Chu et al. 2018). Based on the analysis of SSA, total pore volume, and average pore size, the modification of FMP as a phosphorus source negatively impacts the formation of the biochar pore structure, leading to pore blockage. Conversely, CA-FMP and MCP have a positive effect on the number and distribution of pores by providing alkali metals and H⁺, thereby facilitating pore formation during pyrolysis (Chu et al. 2018). Consequently, CBC and MBC exhibit larger SSA and total pore volume compared to BC, with a smaller average pore diameter. This results in an increased number of potential Cd(II) adsorption sites within the biochar pores, serving as a crucial basis for phosphorus

modification to significantly enhance Cd(II) removal capacity. Additionally, The presence of a superior pore structure not only prevents the loss of internal active sites inside biochar during desorption and adsorption processes but also contributes to enhanced stability and regeneration performance (Fig. S2).

Analysis of adsorption capacity and contribution ratio

The quantitative analysis of the adsorption capacity of PBC for Cd(II) and the contribution ratio of different mechanisms showed that the affinity of biochar for Cd(II) was enhanced by phosphorus modification. The removal rates of FBC, CBC and MBC were 29.15%, 89.73%, and 69.08%, respectively (Fig. 9a). Compared to BC, the adsorption capacity of Cd(II) by mineral components (Q_i+Q_m) in PBC is significantly increased, which is consistent with previous research results (Ge et al. 2022). A small amount of water-soluble calcium and magnesium ions in FMP was successfully loaded onto biochar to increase the ion exchange contribution of FBC; its Q_i contributed the highest proportion (53.15%), which was the same as BC. The adsorption contributions of Q_m of CBC and MBC were the highest (51.10% and 47.98%) (Fig. 9b). Although phosphorus content of CBC is lower than that of MBC, the Q_m of CBC is higher than that of MBC, which is due to the fact that citric acid activates FMP, forming soluble Or-P composition with higher proportion and more uniform phosphorus distribution, and more Ca(II), Mg(II), CO_3^{2-} , and SiO_3^{4-} loaded on the biochar surface. The function of CA also includes reducing the size of biomass, forming rich pore structures, and increase Q_o .

In addition, CBC and MBC are greater than BC, possibly because the presence of inorganic metals and phosphate-based substances promotes the break of chemical bonds and generates more OFGs (Chu et al. 2018; Feng et al. 2018).

Conclusions

PBC exhibits excellent adsorption capacity for heavy metals while posing a low risk of eutrophication. Chemisorption and intra-particle diffusion play crucial roles in the adsorption kinetics. The adsorption of Cd(II) by PBC involves various mechanisms, including ion exchange, mineral precipitation, OFG complexation, cation- π interaction, electrostatic interaction, and physical adsorption. Ion exchange is the primary mechanism for Cd(II) adsorption by BC and FBC, accounting for 51.53% and 53.15% of the adsorption, respectively. On the other hand, mineral precipitation is the main influencing factor for Cd(II) adsorption by CBC and MBC. The maximum adsorption capacity of CBC and MBC is 7.86 and 6.84 times that of BC, respectively, accounting for 51.10% and 47.98% of the total adsorption capacity. The activation of CA improves the pore structure of CBC, resulting in a more uniform distribution of abundant phosphorus, calcium, magnesium, and silicon on its surface. This enhancement contributes to CBC exhibiting the highest removal rate (89.73%). Our results demonstrate that utilizing low-grade phosphate ore and its derivatives as exogenous phosphorus to prepare PBC yields excellent performance. PBC can effectively and reliably serve as an adsorbent to remove heavy metals from polluted water.

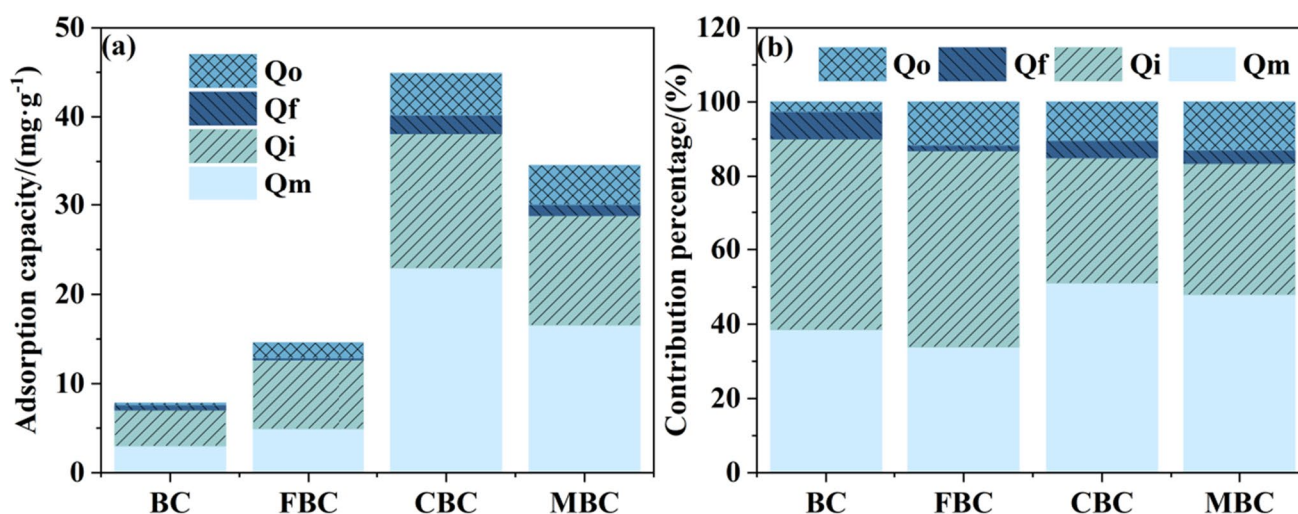


Fig. 9 Adsorption capacity (a) and adsorption contribution ratio (b) of biochars for Cd(II). Note: Q_i , Q_m , Q_f , and Q_o respectively represent the adsorption amounts produced by ion exchange, mineral precipitation, functional group complexation, and other mechanisms

Supplementary Information The online version contains supplementary material available at <https://doi.org/10.1007/s11356-024-32308-y>.

Author contribution Yang Zeng (first author): conceptualization, methodology, software, investigation, formal analysis, and writing—original draft. Yuhan Lin: data curation—original draft. Ming Ma: visualization and writing—review and editing. Hong Chen (corresponding author): conceptualization, funding acquisition, resources, supervision, and writing—review and editing. All authors commented on previous versions of the manuscript. All authors read and approved the final manuscript.

Funding This study was supported by the Chongqing Graduate Scientific Research Innovation Project (CYB22212).

Data Availability The datasets used and/or analyzed during the current study are available from the corresponding author on reasonable request. All data generated or analyzed during this study are included in this published article and its supplementary information files.

Declarations

Ethics approval Not applicable.

Consent to participate Not applicable.

Consent for publication All authors consent when it is submitted.

Competing interests The authors declare no competing interests.

References

- Bekiaris G, Peltre C, Jensen LS, Bruun S (2016) Using FTIR-photoacoustic spectroscopy for phosphorus speciation analysis of biochars. *Spectrochim Acta, Part A* 168:29–36. <https://doi.org/10.1016/j.saa.2016.05.049>
- Bruun S, Harmer SL, Bekiaris G, Christel W, Zuin L, Hu Y, Jensen LS, Lombi E (2017) The effect of different pyrolysis temperatures on the speciation and availability in soil of P in biochar produced from the solid fraction of manure. *Chemosphere* 169:377–386. <https://doi.org/10.1016/j.chemosphere.2016.11.058>
- Chen Y, Li M, Li Y, Liu Y, Chen Y, Li H, Li L, Xu F, Jiang H, Chen L (2021) Hydroxyapatite modified sludge-based biochar for the adsorption of Cu(2+) and Cd(2+): Adsorption behavior and mechanisms. *Bioresour Technol* 321:124413–124422. <https://doi.org/10.1016/j.biortech.2020.124413>
- Chu G, Zhao J, Huang Y, Zhou D, Liu Y, Wu M, Peng H, Zhao Q, Pan B, Steinberg CEW (2018) Phosphoric acid pretreatment enhances the specific surface areas of biochars by generation of micropores. *Environ Pollut* 240:1–9. <https://doi.org/10.1016/j.envpol.2018.04.003>
- Cui X, Fang S, Yao Y, Li T, Ni Q, Yang X, He Z (2016) Potential mechanisms of cadmium removal from aqueous solution by *Canna indica* derived biochar. *Sci Total Environ* 562:517–525. <https://doi.org/10.1016/j.scitotenv.2016.03.248>
- Cui H, Dong T, Hu L, Xia R, Zhou J, Zhou J (2022) Adsorption and immobilization of soil lead by two phosphate-based biochars and phosphorus release risk assessment. *Sci Total Environ* 824:153957–153965. <https://doi.org/10.1016/j.scitotenv.2022.153957>
- Deng Y, Huang S, Laird D, Wang X, Meng Z (2019) Adsorption behaviour and mechanisms of cadmium and nickel on rice straw biochars in single- and binary-metal systems. *Chemosphere* 218:308–318. <https://doi.org/10.1016/j.chemosphere.2018.11.081>
- Deng Y, Huang S, Dong C, Meng Z, Wang X (2020) Competitive adsorption behaviour and mechanisms of cadmium, nickel and ammonium from aqueous solution by fresh and ageing rice straw biochars. *Bioresour Technol* 303:122853–122861. <https://doi.org/10.1016/j.biortech.2020.122853>
- Feng D, Zhang Y, Zhao Y, Sun S (2018) Catalytic effects of ion-exchangeable K+ and Ca2+ on rice husk pyrolysis behavior and its gas–liquid–solid product properties. *Energy* 152:166–177. <https://doi.org/10.1016/j.energy.2018.03.119>
- Gao R, Fu Q, Hu H, Wang Q, Liu Y, Zhu J (2019) Highly-effective removal of Pb by co-pyrolysis biochar derived from rape straw and orthophosphate. *J Hazard Mater* 371:191–197. <https://doi.org/10.1016/j.jhazmat.2019.02.079>
- Ge Q, Tian Q, Wang S, Zhang J, Hou R (2022) Highly efficient removal of lead/cadmium by phosphoric acid-modified hydrochar prepared from fresh banana peels: adsorption mechanisms and environmental application. *Langmuir* 38:15394–15403. <https://doi.org/10.1021/acs.langmuir.2c02693>
- Ho YS, McKay G (1999) Pseudo-second order model for sorption processes. *Process Biochem* 34:451–465. [https://doi.org/10.1016/s0032-9592\(98\)00112-5](https://doi.org/10.1016/s0032-9592(98)00112-5)
- Hou C, Miao J, Gu S, Wang H, Wang Y, Xu X (2019) Innovation of fused calcium magnesium phosphate products to promote industry development. *J Plant Nutr Fert* 25:2162–2169. <https://doi.org/10.11674/zwyf.19172>
- Huang R, Fang C, Lu X, Jiang R, Tang Y (2017) Transformation of phosphorus during (hydro)thermal treatments of solid bio-wastes: reaction mechanisms and implications for P reclamation and recycling. *Environ Sci Technol* 51:10284–10298. <https://doi.org/10.1021/acs.est.7b02011>
- Huang K, Hu C, Tan Q, Yu M, Shabala S, Yang L, Sun X (2022) Highly efficient removal of cadmium from aqueous solution by ammonium polyphosphate-modified biochar. *Chemosphere* 305:135471–135478. <https://doi.org/10.1016/j.chemosphere.2022.135471>
- Lang L, Wang B, Liu T, Wang J, Zhu L, Liu Y, Niu Y (2023) Homogeneous synthesis of Schiff base modified PAMAM dendrimers/silica for efficient adsorption of Hg(II). *Chem Eng J* 477:147310. <https://doi.org/10.1016/j.cej.2023.147310>
- Liu T, Lawluyv Y, Shi Y, Ighalo J, He Y, Zhang Y, Yap P (2022) Adsorption of cadmium and lead from aqueous solution using modified biochar: a review. *J Environ Chem Eng* 10:106502–106533. <https://doi.org/10.1016/j.jece.2021.106502>
- Meng X, Hu R (2021) Nitrogen/phosphorus enriched biochar with enhanced porosity activated by guanidine phosphate for efficient passivation of Pb(II), Cu(II) and Cd(II). *J Mol Liq* 323:115071–115082. <https://doi.org/10.1016/j.molliq.2020.115071>
- Shang H, Li Y, Liu J, Wan Y, Feng Y, Yu Y (2020) Preparation of nitrogen doped magnesium oxide modified biochar and its sorption efficiency of lead ions in aqueous solution. *Bioresour Technol* 314:123708–123715. <https://doi.org/10.1016/j.biortech.2020.123708>
- Shrestha R, Ban S, Devkota S, Sharma S, Joshi R, Tiwari A, Kim H, Joshi M (2021) Technological trends in heavy metals removal from industrial wastewater: a review. *J Environ Chem Eng* 9:105688–105705. <https://doi.org/10.1016/j.jece.2021.105688>
- Sun K, Qiu M, Han L, Jin J, Wang Z, Pan Z, Xing B (2018) Speciation of phosphorus in plant- and manure-derived biochars and its dissolution under various aqueous conditions. *Sci Total Environ* 634:1300–1307. <https://doi.org/10.1016/j.scitotenv.2018.04.099>
- Wang J, Guo X (2022) Rethinking of the intraparticle diffusion adsorption kinetics model: interpretation, solving methods and

- applications. *Chemosphere* 309:136732–136745. <https://doi.org/10.1016/j.chemosphere.2022.136732>
- Wang Q, Duan C, Xu CY, Geng Z (2022) Efficient removal of Cd(II) by phosphate-modified biochars derived from apple tree branches: processes, mechanisms, and application. *Sci Total Environ* 819:152876–152887. <https://doi.org/10.1016/j.scitotenv.2021.152876>
- Wang B, Wu K, Liu T, Cheng Z, Liu Y, Liu Y, Niu Y (2023) Feasible synthesis of bifunctional polysilsesquioxane microspheres for robust adsorption of Hg(II) and Ag(I): behavior and mechanism. *J Hazard Mater* 442:130121. <https://doi.org/10.1016/j.jhazmat.2022.130121>
- Wu J, Wang T, Wang J, Zhang Y, Pan WP (2021) A novel modified method for the efficient removal of Pb and Cd from wastewater by biochar: enhanced the ion exchange and precipitation capacity. *Sci Total Environ* 754:142150–142159. <https://doi.org/10.1016/j.scitotenv.2020.142150>
- Xu X, Hou C, Wang H, Tang J (2010) Structure of phosphate-containing aluminosilicate vitreous body of complex components with low chemical stability: model of phosphate-containing aluminosilicate vitreous structure and fertilizer development. *Sci China: Chem* 40:922–926. <https://doi.org/10.1360/zb2010-40-7-922>
- Yang F, Lv J, Zhou Y, Wu S, Sima J (2023) Co-pyrolysis of biomass and phosphate tailing to produce potential phosphorus-rich biochar: efficient removal of heavy metals and the underlying mechanisms. *Environ Sci Pollut Res* 30:17804–17816. <https://doi.org/10.1007/s11356-022-23128-z>
- Yu Y, Du C (2023) A review on the P enrichment and recovery from steelmaking slag: towards a sustainable P supply and comprehensive utilization of industrial solid wastes. *Sci Total Environ* 891:164578–164591. <https://doi.org/10.1016/j.scitotenv.2023.164578>
- Yu Y, Liu D, Wu H (2013) Formation and characteristics of reaction intermediates from the fast pyrolysis of NaCl- and MgCl₂-loaded celluloses. *Energy Fuels* 28:245–253. <https://doi.org/10.1021/ef401483u>
- Yuan Q, Wang P, Wang X, Hu B, Wang C, Xing X (2023) Nano-chlorapatite modification enhancing cadmium(II) adsorption capacity of crop residue biochars. *Sci Total Environ* 865:161097–161107. <https://doi.org/10.1016/j.scitotenv.2022.161097>
- Zamora-Ledezma C, Negrete-Bolagay D, Figueroa F, Zamora-Ledezma E, Ni M, Alexis F, Guerrero V (2021) Heavy metal water pollution: a fresh look about hazards, novel and conventional remediation methods. *Environ Technol Innovation* 22:101504–101529. <https://doi.org/10.1016/j.eti.2021.101504>
- Zhang S, Zhang H, Cai J, Zhang X, Zhang J, Shao J (2017) Evaluation and prediction of cadmium removal from aqueous solution by phosphate-modified activated bamboo biochar. *Energy Fuels* 32:4469–4477. <https://doi.org/10.1021/acs.energyfuels.7b03159>
- Zhang A, Li X, Xing J, Xu G (2020a) Adsorption of potentially toxic elements in water by modified biochar: a review. *J Environ Chem Eng* 8:104196–104205. <https://doi.org/10.1016/j.jece.2020.104196>
- Zhang H, Shao J, Zhang S, Zhang X, Chen H (2020b) Effect of phosphorus-modified biochars on immobilization of Cu (II), Cd (II), and As (V) in paddy soil. *J Hazard Mater* 390:121349–121356. <https://doi.org/10.1016/j.jhazmat.2019.121349>
- Zhang H, Ke S, Xia M, Bi X, Shao J, Zhang S, Chen H (2021) Effects of phosphorous precursors and speciation on reducing bioavailability of heavy metal in paddy soil by engineered biochars. *Environ Pollut* 285:117459–117469. <https://doi.org/10.1016/j.envpol.2021.117459>
- Zhang H, Liao W, Zhou X, Shao J, Chen Y, Zhang S, Chen H (2022a) Coeffect of pyrolysis temperature and potassium phosphate impregnation on characteristics, stability, and adsorption mechanism of phosphorus-enriched biochar. *Bioresour Technol* 344:126273–126282. <https://doi.org/10.1016/j.biortech.2021.126273>
- Zhang Z, Li Y, Zong Y, Yu J, Ding H, Kong Y, Ma J, Ding L (2022b) Efficient removal of cadmium by salts modified-biochar: performance assessment, theoretical calculation, and quantitative mechanism analysis. *Bioresour Technol* 361:127717–127728. <https://doi.org/10.1016/j.biortech.2022.127717>
- Zhang K, Yi Y, Fang Z (2023) Remediation of cadmium or arsenic contaminated water and soil by modified biochar: a review. *Chemosphere* 311:136914–136928. <https://doi.org/10.1016/j.chemosphere.2022.136914>
- Zhao X, Cai M, Dong Q, Li Y, Sheng J (2018) Advances of mechanisms and technology pathway of efficient utilization of medium-low grade phosphate rock resources. *J Plant Nutr Fert* 24:1121–1130. <https://doi.org/10.11674/zwyf.17418>
- Zhou X, Xu D, Yang J, Yan Z, Zhang Z, Zhong B, Wang X (2023) Treatment of distiller grain with wet-process phosphoric acid leads to biochar for the sustained release of nutrients and adsorption of Cr(VI). *J Hazard Mater* 441:129949. <https://doi.org/10.1016/j.jhazmat.2022.129949>

Publisher's Note Springer Nature remains neutral with regard to jurisdictional claims in published maps and institutional affiliations.

Springer Nature or its licensor (e.g. a society or other partner) holds exclusive rights to this article under a publishing agreement with the author(s) or other rightsholder(s); author self-archiving of the accepted manuscript version of this article is solely governed by the terms of such publishing agreement and applicable law.